Heliyon 9 (2023) e17010

Contents lists available at ScienceDirect

Heliyon

journal homepage: www.cell.com/heliyon

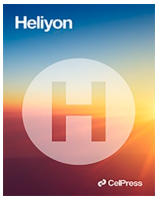

Establishment of a multifunctional impact system and a study of a pancreatic trauma model in rats based on controlling the injury area

Wang Hailin [a,1], Han Li [b,1], Zhao Zhirong [c], Wang Qingqing [c], Li Jingdong [a], Dai Ruiwu [c,*]

[a] Department of Hepatobiliary Surgery, Affiliated Hospital of North Sichuan Medical College, Nanchong, Sichuan Province, China
[b] Ultrasonography Department, Sichuan Clinical Research Center for Cancer, Sichuan Cancer Hospital & Institute, Sichuan Cancer Center, Affiliated Cancer Hospital of University of Electronic Science and Technology of China, Chengdu, China
[c] General Surgery Center, General Hospital of Western Theater Command, Chengdu, Sichuan Province, China

ARTICLE INFO

Keywords:
Impactor
Pancreatic trauma
Model
Injury area

ABSTRACT

Background: At present, basic scientific research on pancreatic trauma is rare due to the lack of ideal animal models and modeling equipment for pancreatic trauma. Therefore, we intend to develop a multifunctional impact system with simple operation, diverse impact and accurate measurement and to establish a rat pancreatic trauma model based on injury area control by using the system.

Methods: The impactor was designed based on the convenience of the impact energy acquisition, the diversity of the impact operation, and the precision of the impact strength parameter measurement by the team. The efficacy and stability/repeatability of the impactor were preliminarily evaluated. An impact head with different impact areas (3 cm^2 and 6 cm^2) of the impactor was used to squeeze the rat pancreas in the abdomen to form different injury areas under a pressure of 400 kPa. The efficacy features of this trauma model were evaluated by detecting the outcomes of pathology and biochemistry at 24 h after injury in the two groups. Furthermore, these changes were also evaluated at 6 h, 24 h, 48 h and 72 h after injury in the 3 cm^2 trauma group.

Result: Multifunctional impactors were successfully explored. The impact force was continuously adjustable with a range of 0–200 kg. The compression and extrusion stress ranges were continuously adjustable from 0 to 100 kg. System adjustment verified that the impactor had fine efficacy ($P < 0.05$) and stability/repeatability ($P > 0.05$). Compared with the control group, rats in the pancreatic trauma group with different injury areas exhibited obvious injuries ($P < 0.05$), and compared with the 3 cm^2 trauma group, the 6 cm^2 trauma group exhibited the more severe injury ($P < 0.05$). After modeling, the injury characteristics at different time points showed stable differences($P < 0.05$).

Conclusions: A rat pancreatic trauma model based on injury area control was successfully established using the impactor developed in this study. This model is simple, effective, controllable, and suitable for animal experimental research on pancreatic trauma.

* Corresponding author.
E-mail address: dairuiwu@swjtu.edu.cn (D. Ruiwu).
[1] These authors contributed equally to this study.

https://doi.org/10.1016/j.heliyon.2023.e17010
Received 20 April 2022; Received in revised form 26 May 2023; Accepted 4 June 2023
Available online 11 June 2023

1. Background

In recent years, the incidence of pancreatic trauma has increased due to an increase in accidents, falls, hard hits, earthquake disasters, gas explosions in mines, boiler explosions, military blast injuries, and wartime injuries [1,2]. As a retroperitoneal organ, the pancreas is located behind multiple organs. Due to its special anatomical position, it is difficult to identify injury, which delays treatment time and confers a high mortality rate [3]. Furthermore, a posttraumatic reinjury effects will occur because the pancreas produces many digestive enzymes [4]. In addition, systemic complications easily occur, which are often life threatening [5]. Therefore, research on effectively inhibiting pancreatic tissue damage and promoting pancreatic cellular repair is an important and urgent topic in the field of trauma surgery.

Currently, clinical studies on pancreatic trauma have focused on injury assessment and treatment strategies based on the American Association for the Surgery of Trauma (AAST) pancreatic trauma grading scale [6]. However, basic scientific research of pancreatic trauma is rare due to the lack of ideal animal models and modeling equipment for pancreatic trauma. Acquiring more information on the pathophysiology, pathology, cell biology and molecular biology of pancreatic trauma may contribute to further research on diagnosis and treatment of pancreatic trauma. Although many impact systems have been established, they have limited applicability and several shortcomings such as large equipment size, complex operation, inconvenient handling and high cost, making it difficult to accurately simulate injury in experimental animal models [7–9]. In the past, only air impact or air pressure could be adjusted, and the injury area was only controlled within 0.5–1 cm^2. It was not applicable to the research of organ large area damage after a single impact [10,11]. Therefore, we intend to develop a multifunctional impact system with simple operation, diverse impact and accurate measurement and to evaluate its function in an animal injury model in this study. In addition, we intend to explore a new pancreatic trauma model in rats based on different injury areas control by using the system and to evaluate trauma features of this model by detecting the outcomes of pathology and biochemistry.

2. Methods

2.1. The multifunctional impact system

Our team developed the impact system, the equipment has an authorized patent (self-developed, patent number: ZL 2016 1 0347341.5), and the design is shown in Fig. 1. The impact system consists of an energy storage device (marked 2, 3, 4, 9, and 10 in Fig. 1), a multifunctional impact device (marked 5, 6, 7, and 8 in Fig. 1) and a parameter measurement device (marked 1, 11, 12, 13, 14, and 15 in Fig. 1). The parameter measurement device was purchased from Shenzhen COOPERATION Sensors Instrument CO., Ltd. The other devices were manufactured by Chengdu Tuanjie Mould Casting Company and Chengdu Guanghua Rubber Co., Ltd.

2.2. Instrument parameters and impact parameters

The impactor was 450 mm × 450 mm × 800 mm in volume and weighed approximately 60 kg (Fig. 2A). The specification of a spring was matched with a cylinder with a scale slot. At present, the impactor has a group of spring of 4–8 mm wire diameter and a cylinder with a scale slot of 80 mm inner diameter. The peak value of impact stress adjustable range is 0–200 kg, and the compressive stress adjustable range is 0–100 kg (Fig. 2B). The impact head has two kinds of materials, hard metal and flexible plastic, and the impact area is 3–8 cm^2 for selection. In addition, the impact head was designed in fan shape, round and other shapes (Fig. 2C). The induction range of the pressure sensor probe is 0–200 kg (Fig. 2D).

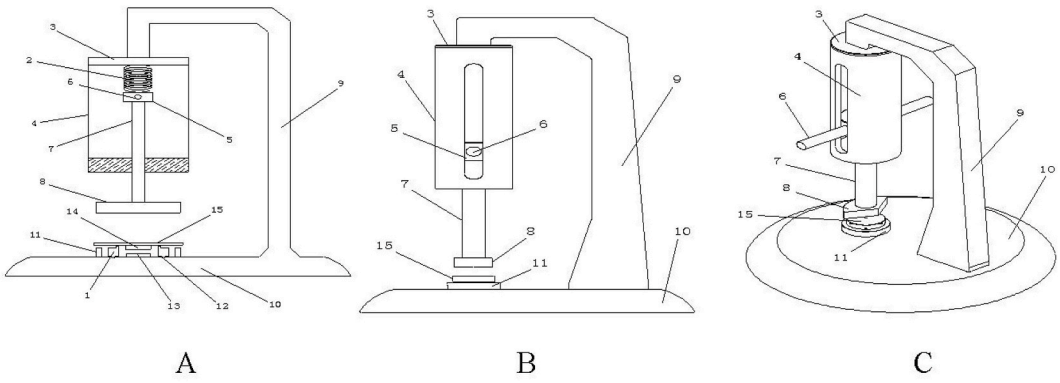

Fig. 1. Design of the Multifunctional Impactor. A, B and C: the internal structure schematic diagram, sagittal schematic diagram and three-dimensional appearance schematic diagram of the impactor. The corresponding digital components in A, B, and C are as follows: 1-pressure sensor probe, 2-spring, 3-top cover with rubber pad, 4-cylinder with scale slot, 5-spring compression base, 6-operating rod, 7-impact rod, 8-adjustable impact head, 9-support frame, 10-base, 11-ring column, 12-screw slot, 13-cylinder table, 14-thread boss, 15-pad.

2.3. The impact principle and application of multifunctional impactor

In a complete impact operation process, the spring is compressed by pulling the operating rod (handle rod) in the energy storage device to produce elastic potential energy, and the elastic potential energy is converted into kinetic energy while the operating rod is released. Different combinations of spring mechanical parameters determine the different impact stress ranges of the device. The multifunctional impact device includes different sizes and shapes of the impact head used to control the contact mode and impact area of the impact, allowing adjustment of the impact angle and alteration of the impact head to meet the needs of different impact conditions. The parameter measuring device that measures the impact primarily depends on the pressure sensor to measure and display the impact stress value.

2.4. The validity/efficacy and stability/repeatability detection of impactor

First, the efficacy of the impactor was tested. Three sets of springs with the same impact mechanical parameters were selected and distributed into 3 groups, and the impact was performed according to the standard compression length of springs of 10 cm, 20 cm, and 30 cm respectively. Each group was continuously impacted 10 times and the impact parameters (compression stress and impact stress) were recorded. Then, the stability/repeatability of the impact instrument was tested. The above specific spring was assembled in the impact instrument, and an impact standard with a compression length equal to 20 cm was set. The number of operation times, the corresponding compression stress value, and the peak value of impact stress were recorded. According to this impact standard, more than 510 impacts were repeated. Data from 1 to 10 times, 101–110 times, 301–310 times, and 501–510 times were divided into four groups, and the average value of impact parameters was taken for each group. The coefficient of variation (CV) of different strike frequency range was evaluated. $CV = s/\bar{x} \times 100\%$.

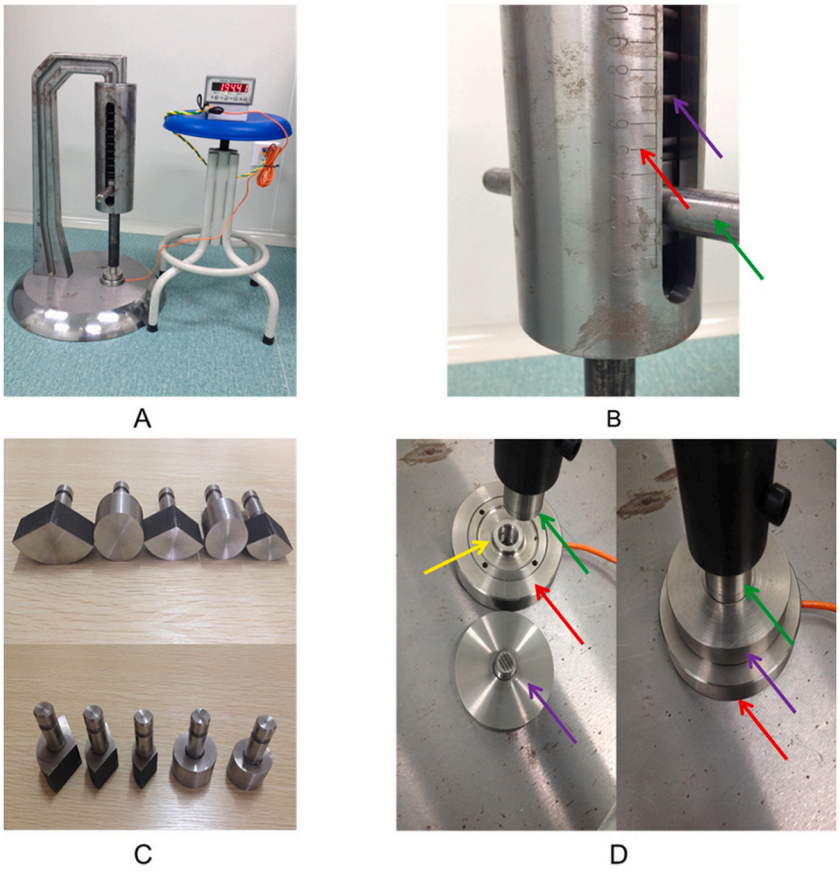

Fig. 2. The whole device and each component of the multifunctional impactor. A: the whole of the impactor. B: the primary components of the energy storage device (the red arrow is cylinder with scale groove, and the green arrow is operating rod, and the purple arrow is spring). C: the impact head with different shapes and impact area. D: the primary component of the parameter measurement device (red, green, purple, yellow arrows show ring column, adjustable impact head, pad, pressure sensor probe).

2.5. Animals and reagents

SD rats (adult male, SPF grade, weight 250 ± 10 g) were obtained from Chengdu Dashuo Laboratory Animal Co., Ltd, and care was provided according to the guidelines of the Institutional of Animal Care and Use Committee. The HE kit, potassium test kit, calcium test kit, amylase test kit and lipase test kit were produced from Nanjing Jiancheng Bioengineering Institute. The TUNEL kit was purchased from Promega Company. The enzyme-linked immunosorbent assay (ELISA) kit for the detection of inflammatory factors was purchased from Boster Biological Technology co., Ltd.

2.6. Ethical approval

All experimental programmes of this study were approved and supervised by the Ethics Committee of North Sichuan Medical College. Inhalation aerosol anesthesia was used to relieve animal pain and give animal humanitarian care.

2.7. Animal groups and model establishment

According to our previous experimental study, we established a stable rat model of pancreatic trauma under 400 kPa pressure [10, 11]. Fifty SD rats were randomly divided into 3 groups, including 20 rats in the 3 cm^2 trauma group, 20 rats in the 6 cm^2 trauma group and 10 rats in control group. The pancreases of rats in the 3 cm^2 trauma group and 6 cm^2 trauma group were respectively impacted by 3 cm^2 and 6 cm^2 impact head. Under the same pressure (400 kPa), the impact strengths of the 3 cm^2 trauma group and 6 cm^2 trauma group were 12 kg and 24 kg, respectively. All groups were fasted from water for 12 h and anesthetized. The opening to the abdominal cavity in the median line of the upper abdomen, and spleen and portal vein were regarded as the boundary. Then the pancreas was exposed and separated. In the 3 cm^2 trauma group and 6 cm^2 trauma group, the pancreas is located between the buffer plate and the impact head by moving and adjusting the position of the buffer plate and the impact head. To ensure the formation of blunt injury by simple impact, tearing injury of pancreatic tissue caused by excessive migration of the pancreas is not permitted in the quality control. The pancreas was impacted by the disinfected different areas impact head, and the impact time was 0.5s. In the control group, the pancreas was only flipped several times by a cotton swab and without impact (sham). When impact completion, the general pathological changes in the pancreas area were immediately observed, rats were closed abdomen and continuously observed for 24 h. Further, another 30 rats were randomly divided into 3 subgroups for modeling the 3 cm^2 trauma group, and all subgroups were observed at 6, 48, and 72 h after modeling, respectively. Then, rats were euthanized by abdominal aorta blood collection at the target time points, and the ascites, serum and pancreas of the rats were collected and stored at −80 °C. Related indicators including ascites volume, wet pancreatic weight, pancreatic pathology, pancreatic apoptosis, serum potassium (K^+) and calcium (Ca^{2+}) concentrations, serum inflammatory cytokines levels, and serum and ascites amylase (AMS) and lipase (LPS) activities were measured to assess the trauma model severity. The modeling process is as follows (Fig. 3).

2.8. Rats' condition and pathological changes

After modeling for 24 h, the following conditions were observed in each group, including survival, activity and diet. Anatomical pathological changes were observed by laparotomy.

2.9. Histopathology (HE staining)

Pancreatic tissue was fixed in 4% paraformaldehyde, and HE staining was performed. Histopathological changes were observed under an optical microscope. The same pathologist who was blinded to the experimental group was assigned to score the degree of pathology according to the standard of A Brooks [12] et al. Ten high-power images were taken for each slice, and the final score of a

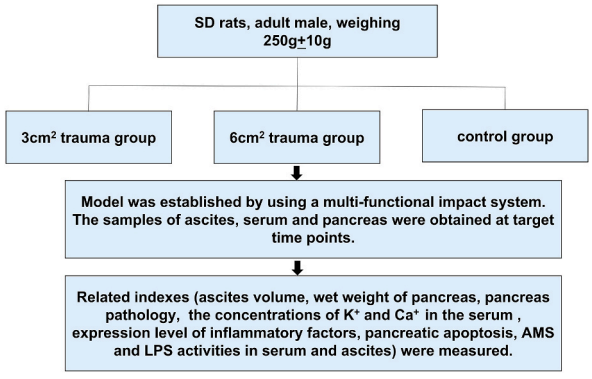

Fig. 3. Animal grouping and modeling processes.

single slice was the average of the scores of ten fields.

2.10. Pancreatic apoptosis detection by TUNEL staining

Pancreatic paraffin sections were stained with TUNEL according to the instructions of the kit, and then the stained sections were observed under a fluorescence microscope at 200 times. The nuclei of the pancreas cells were stained blue by DAPI, and those stained with green fluorescent particles were apoptotic cells. The apoptosis of pancreatic cells were compared in groups. Quantification of apoptotic cells: all slices were observed randomly in 4 high-power visual fields, and the total number of apoptotic cells was counted. Apoptotic index = the total number of apoptotic cells/the total number of pancreatic cells × 100%.

2.11. Biochemical detection

Blood samples were collected from the abdominal aorta. After blood coagulation, samples were centrifuged at 3000 rpm for 5 min at 4 °C. The serum and ascites were stored at −80 °C. Data were detected by spectrophotometry according to the kit instructions, including the concentrations of potassium (K^+) and calcium (Ca^{2+}) in serum and the activities of amylase (AMS) and lipase (LPS) in serum and ascites. Serum inflammatory factors were also detected using ELISA kits.

2.12. Statistical analysis

Statistical analyses were performed in SPSS Version 19.0 and statistical graphs were made by GraphPad Prism. All data were presented as the mean values ± SD and were analyzed using ANOVA or independent-sample *t*-test. The rank sum test was used for nonnormally distributed data. Post-hoc power analysis was performed using GPower3.1. $P < 0.05$ were considered statistically significant.

3. Results

3.1. Detection of impactor validity/efficacy and stability/repeatability

The efficacy test of the impactor showed that the impact parameters (compression stress and impact stress) of the multifunctional impact system were significantly different by adjusting the compression length of the spring (Table 1). The stability/repeatability test of the impactor showed that the compressive stress decreased after more than 300 times impact operations and the impact stress decreased after more than 500 times impact operations (Table 2).

3.2. Survival rate and general changes

The 3 cm^2 trauma group was successfully modeled, after observation for 24 h, 6 rats died due to trauma intolerance, 14 surviving rats were less active and had poorer response to the outside world than normal rats. The 6 cm^2 trauma group was successfully modeled and 9 rats died due to trauma intolerance 24 h later. The behavior and activity of the 11 surviving rats in the 6 cm^2 trauma group were similar to those in the 3 cm^2 trauma group but more serious. One of the rats in the control group died of anesthesia failure, and the remaining 9 survived beyond 24 h. Approximately 10–12 h after modeling, we observed that the behavior of the rats gradually recovered to normal and the rats began to drink water independently in the control group. The survival rates in the 3 cm^2 trauma group and 6 cm^2 trauma group were 70% and 55% at 24 h after modeling, respectively. Further, the 3 cm^2 trauma group demonstrated 100%, 70%, and 60% survival rates at 6, 48 and 72 h, respectively.

3.3. Anatomical pathological changes

(1) After pancreatic extrusion, the pancreas of rats rapidly developed hyperemia and swelling, further, we discovered a small amount of exudation, scattered bleeding, and pancreatic tissue contusion. The injury area of pancreas in the 6 cm^2 trauma group was larger than that in the 3 cm^2 trauma group. The pancreas was pale red, with a clear boundary with the surrounding tissue and there were no other abnormalities in the control group (Fig. 4). (2) After 24 h of modeling, the 3 cm^2 trauma group and 6 cm^2 trauma group exhibited gastrointestinal tract expansion with retention. In addition, red bloody ascites formation occurred, mesenteric and intestinal wall congestion, swelling and exudation were apparent, the adipose tissue exhibited necrotic liquefaction and saponification spots at the root of the mesentery, pancreatic swelling was markedly more severe than 24 h ago. There were no significant changes in the

Table 1
Comparison of impact parameter in different compressed length (n = 10, $\bar{x} \pm s$).

Impact parameters	Compression length of springs = 10 cm	Compression length of springs = 20 cm	Compression length of springs = 30 cm
Compression stress (kg)	7.99 ± 0.72[a]	20.06 ± 0.55[a]	37.91 ± 0.59[a]
Impact stress (kg)	15.18 ± 1.09[#]	40.03 ± 0.84[#]	80.94 ± 2.78[#]

[a] Comparison between groups, $P<0.05$; #: Comparison between groups, $P<0.05$.

Table 2
Comparison of impact parameter in different strike frequency range and the coefficient of variation (CV) of different strike frequency range (n = 10, $\bar{x} \pm s$).

Impact parameters or coefficient of variation (CV)	1-10 times	101-110 times	301-310 times	501-510 times
Compression stress (kg)	20.06 ± 0.55※	20.14 ± 0.58※	19.37 ± 0.63▲	18.94 ± 0.72▲
Impact stress (kg)	40.03 ± 0.84*	39.97 ± 0.88*	39.62 ± 1.02*	35.18 ± 2.08#
CV of Compression stress (%)	2.74	2.88	3.25	3.80
CV of Impact stress (%)	2.10	2.20	2.57	5.91

※, ▲: Compare with same mark, $P>0.05$; Comparison of different markers, $P<0.05$.
*, #: Compare with same mark, $P>0.05$; Comparison of different markers, $P<0.05$.

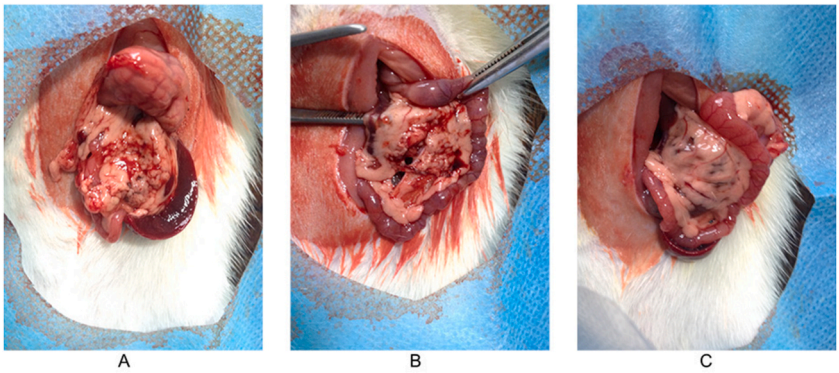

Fig. 4. Immediate damage to the pancreas after impact extrusion. A: the pancreas after modeling in the 3 cm^2 trauma group. B: the pancreas after modeling in the 6 cm^2 trauma group. C: the pancreas in the sham operation group.

control group (Fig. 5). (3) The wet weight of the pancreas and ascites volume in each group and subgroup after injury were shown in Fig. 6A and B.

3.4. Histopathological changes

After 24 h of modeling, the pancreatic parenchymal cell and interstitial cells exhibited varying degrees of congestion, edema, and necrosis (nuclear pyknosis, nuclear fragmentation, and nuclear dissolution). An unequal amount of red blood cell exudation and inflammatory cell infiltration were observed in the tissue. The shape of the glands was altered, some glands were vacuolar and vary in size. There were no obvious pathological changes in the pancreas in the control group. The histopathological changes and pathological score of the pancreas in each group were shown in Fig. 7A and B.

3.5. Apoptosis detection (TUNEL staining)

Under a fluorescence microscope, the nucleus was dyed blue by DAPI, and apoptotic cells showed green (Fig. 8A). After 24 h of

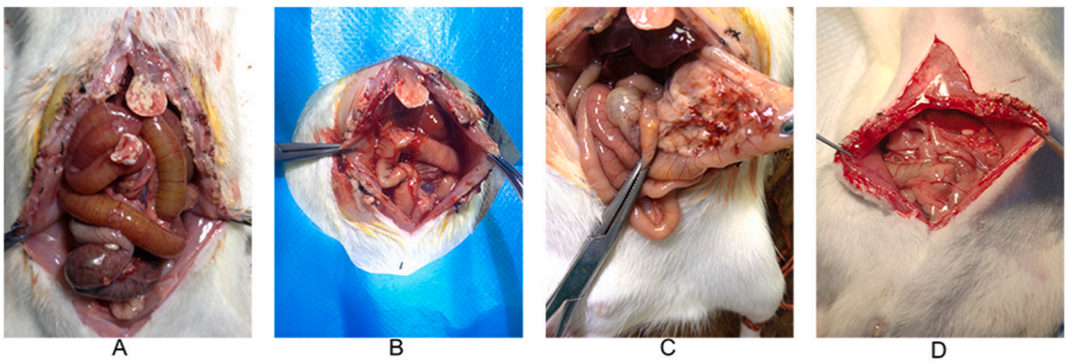

Fig. 5. Anatomical pathology of the pancreas 24 h after trauma. In the trauma group: 1.Gastrointestinal tract expansion with retention, intestinal wall congestion swelling, exudation, abdominal adipose tissue necrosis and saponification spots (A); 2.Abdominal hemorrhagic ascites and blood clots (B); 3.Hemorrhagic necrosis scattered in the pancreas (C). In the sham operation group, no significant change was observed (D).

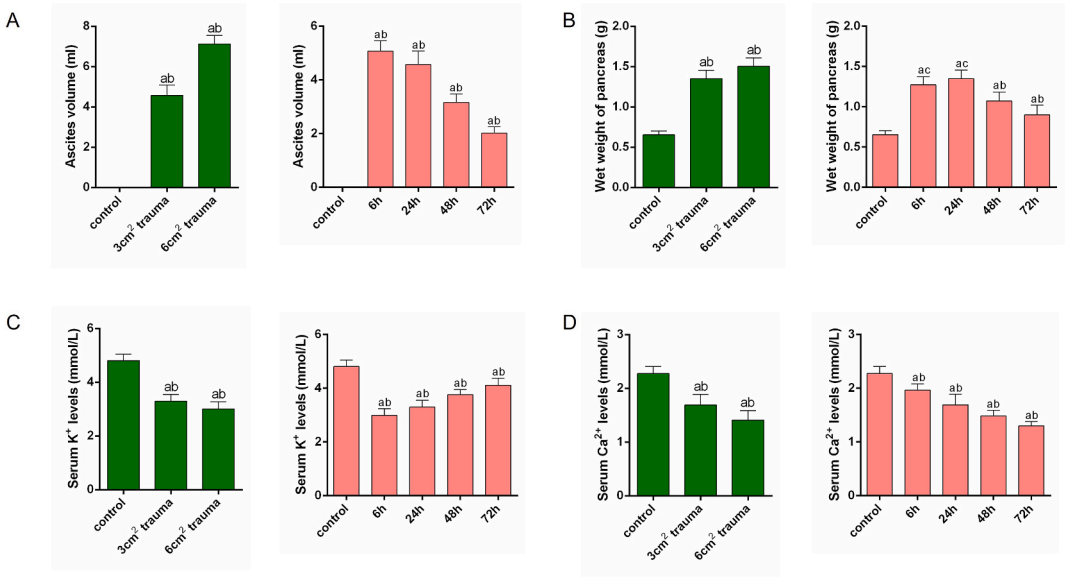

Fig. 6. Changes of relevant indicators after modeling. A, B, C and D were ascites volume, pancreas wet weight, serum potassium and calcium concentrations in each group after modeling, respectively. a: compared with the control group, $P<0.05$; b: comparison of trauma groups with different injury areas or comparison of subgroups at different time points in 3 cm^2 trauma group, $P<0.05$; c: compared with the same labeled group, $P>0.05$.

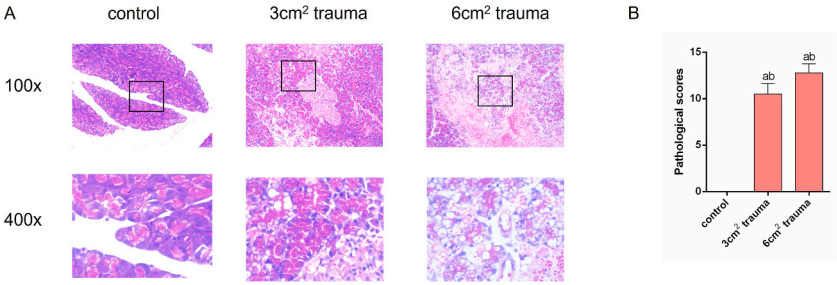

Fig. 7. Histopathological changes 24 h after pancreatic trauma. The 3 cm^2 trauma group pancreas exhibited red blood cell exudation, pancreatic cell destruction and empty bubble, and islet structure was still complete. In the 6 cm^2 trauma group, red blood cell exudation was more obvious, gland cell destruction and vacuole structure were increased, and islet structure had disappeared. Morphological integrity of pancreatic cells and islets in the control group (Fig. 7A). Pathological scores of pancreas were shown in Fig. 7B. a: compared with the control group, $P<0.05$; b: comparison among different trauma groups, $P<0.05$.

modeling, pancreatic apoptosis cells were observed in both the 3 cm^2 trauma group and 6 cm^2 trauma group, and the latter was more serious. The apoptosis indexes of pancreatic cells in groups after trauma were shown in Fig. 8B.

3.6. Biochemical detection

The biochemical indexes demonstrated characteristic changes. Serum potassium (K^+) and calcium (Ca^{2+}) concentrations in each group were shown in Fig. 6C and D. Serum amylase (AMS) and lipase (LPS) activities, and ascites amylase (AMS) and lipase (LPS) activities in each group were shown in Fig. 9A, B, C, and D. Serum inflammatory cytokines levels in groups were shown in Fig. 10A, B, and C.

4. Discussion

With the frequent occurrence of traffic accidents and other accidents in recent years, the number of years of potential life loss (YPLL) of trauma is greater than that of any other disease. Therefore, trauma has increasingly become the focus in the field of surgery [13,14]. The pancreas is a retroperitoneal organ with important functions of internal and external secretion. In addition to its rich blood vessel supply, it also contains easily activated digestive enzymes. Therefore, pancreatic leakage, bleeding, infection, and other complications are more likely to occur after trauma [15–17]. Therefore, pancreatic trauma is complicated and difficult to treat. It is a

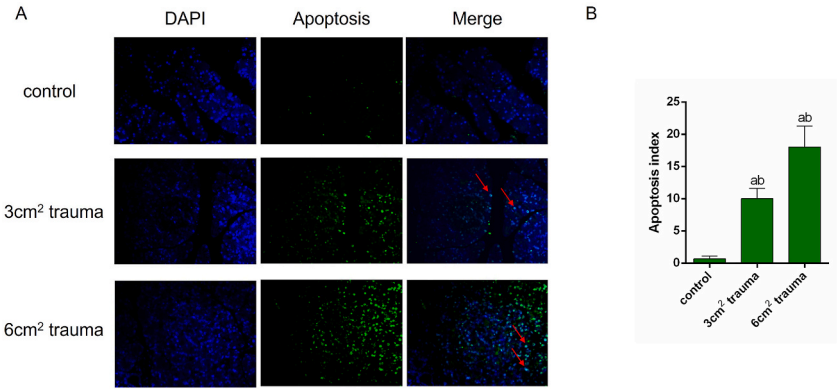

Fig. 8. Apoptosis of pancreatic cells at 24 h after modeling (× 400). At 24 h after modeling, apoptotic pancreatic cells (indicated by the red arrow) were observed in both the 3 cm^2 trauma and 6 cm^2 trauma groups, with the latter being more severe (Fig. 8A). The apoptotic index was shown in Fig. 8B. a: compared with the control group, $P<0.05$; b: comparison among different trauma groups, $P<0.05$.

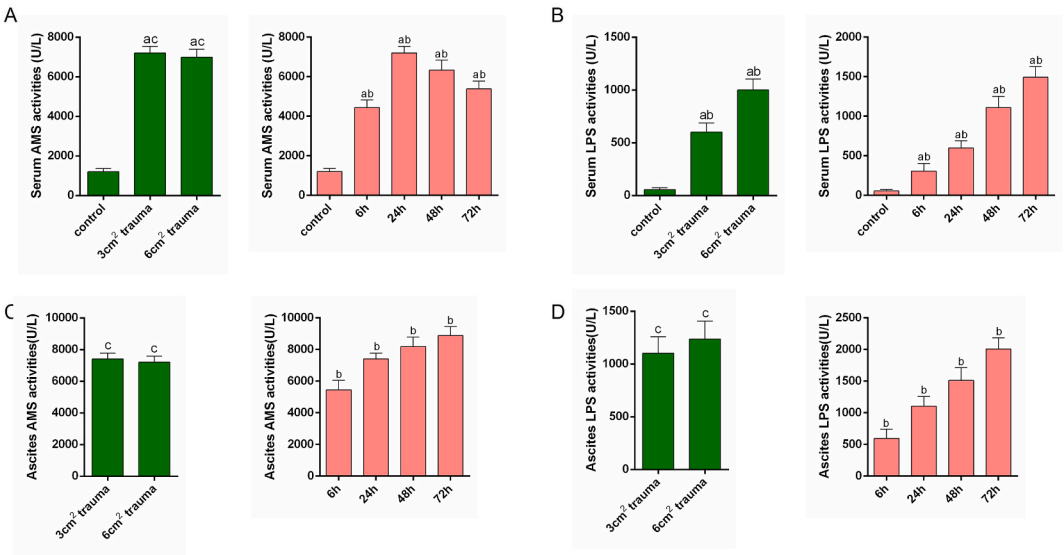

Fig. 9. Pancreatin levels in each group after modeling. A, B, C and D were serum amylase, lipase and ascites amylase and lipase, respectively. As there were no ascites samples in the control group, there were no control data in C and D. a: compared with the control group, $P<0.05$; b: comparison of trauma groups with different injury areas or comparison of subgroups at different time points in 3 cm^2 trauma group, $P<0.05$; c: compared with the same labeled group, $P>0.05$.

prerequisite for the study of trauma-related subjects to establish animal models that can imitate the physiological and pathological characteristics of pancreatic trauma in humans. The model is important to explore the injury mechanism, pathology, and injury evolution in order to propose ways to reduce or avoid secondary injury to tissues and organs. For this aim, we developed an impactor and established a model based on the control of different injury areas to simulate different grades of human pancreatic trauma. The model of rats has satisfactory survival rates and stable, differentiated blunt pancreatic injury.

Our impactor has the following characteristics: (1) It ensures that the impact stress is adjusted in a large range. (2) The type and material of the impact head ensures that the characteristics and scope of the damage are controlled and that the damaged area is stable. (3) The pressure sensor system reliably measures the impact parameters. (4) The impactor is low cost, has good operational safety, and is easy to transport. We first verified the efficacy of the impactor (Table 1). The corresponding impact parameters show stable difference under different compression length of spring, indicating that the impactor can better control the impact parameters to suit the experimental impact requirements. Then, the stability/repeatability of the impact system was tested (Table 2). With increasing impact times, the impact parameters showed a stable difference. The compressive stress and impact stress began to decrease, and the CV value increased after more than 300 and 500 cycles respectively, indicating that the stability of the impactor began to decrease. Therefore, during impact operation within 300 cycles, the impact parameters exhibited good stability. When the impact times exceeded this threshold, system errors increased, and the stability worsened due to the change in spring metal fatigue and mechanical parameters. A suggested solution to this issue is to replace the spring to ensure stability of the impactor, when the cumulative impact times reaches

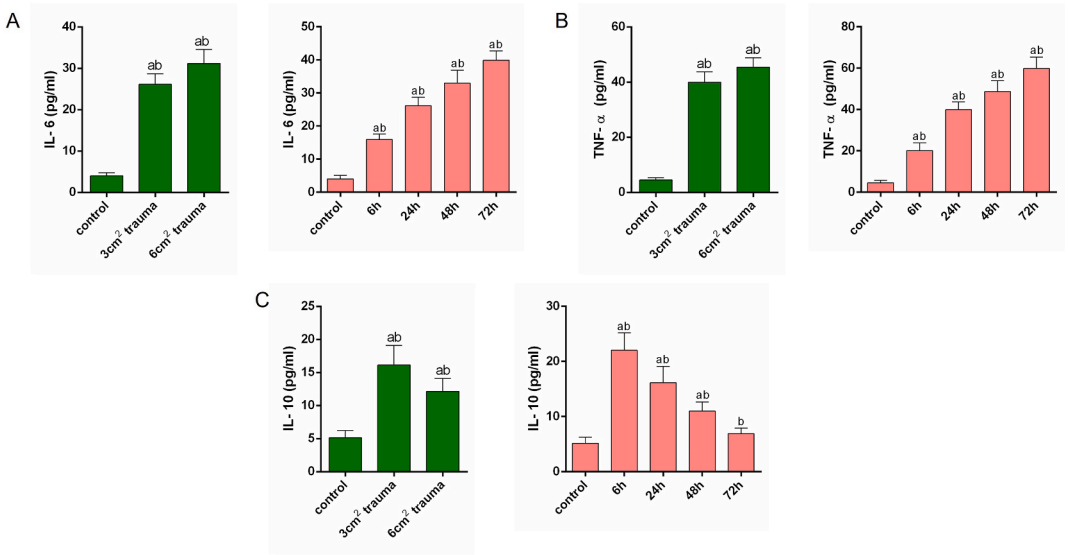

Fig. 10. Serum inflammatory cytokine levels in each group after modeling. A, B and C were IL-6, TNF-α and IL-10 levels, respectively. a: compared with the control group, $P < 0.05$; b: comparison of trauma groups with different injury areas or comparison of subgroups at different time points in 3 cm^2 trauma group, $P < 0.05$.

300.

There are two primary standards for establishing a successful trauma model: one is to ensure the survival of experimental animals after trauma within the research time range, and the other is the formation of target trauma [9]. Based on previous studies, we verified that 400 kpa and 1 cm^2 impact parameters caused obvious pancreatic trauma in rats and that these rats maintained a high survival rate [10,11]. However, since the goal of establishing animal models is to simulate clinical trauma as much as possible, the above animal models also have shortcomings that cannot recapitulate extensive pancreatic trauma. Therefore, we designed a pancreatic crush injury model with different area using 3 cm^2 and 6 cm^2 impact head (30% and 60% of the total area of the pancreas) in this study. At the same time, the injury mechanism primarily manifests as less vascular injury and more severe pancreatic tissue injury, so the model has characteristics of simplicity concerning injury factors, controllable injury range, and good stability.

These results showed that: (1)At 24 h after modeling, the survival rate and general condition of rats in the two experimental groups were significantly lower than those in the control group, and the mortality rate in 6 cm^2 trauma group was higher than in 3 cm^2 trauma group. Further, The survival rates of 3 cm^2 trauma subgroups were gradually decreased at 6, 24, 48, and 72 h (2)At 24 h after modeling, the ascites volume, pancreatic wet weight, pathological score, apoptosis index, and pro-inflammatory factors (IL-6, TNF-α) levels were higher in 6 cm^2 trauma group than in 3 cm^2 trauma group, and there was more bleeding and necrosis in 6 cm^2 trauma group. These pathological changes indicated that damage was more serious in response to the increase in pancreatic impact area. (3) At 24 h after modeling, there were significant differences in serum K^+ and Ca^{2+} between the two groups, and with the increase in trauma area, K^+ and Ca^{2+} gradually decreased. The reason may be that additional K^+ and Ca^{2+} were lost in ascites after pancreatic trauma. Additionally, high trypsin levels were released after pancreatic cells were injured, and trypsin decomposed the adipose tissue around the pancreas into fatty acids. The latter was then combined with Ca^{2+} to form saponification spots, which might be another possible reason for this observation [18,19]. (4) At 24 h after modeling, amylase in serum and ascites of trauma groups were significantly higher than in the control group, but there was no significant difference between 3 cm^2 and 6 cm^2 trauma groups. There was a significant difference in serum lipase activity between trauma groups and the control group. There was a significant difference in serum lipase activity between the trauma groups, while there was no significant difference in ascites lipase activity between trauma groups. Further, the findings showed that amylase and lipase in serum and ascitic fluid were significantly different at 6, 24, 48, and 72 h time points in 3 cm^2 trauma subgroups after modeling. Therefore, the activity levels of amylase and lipase at a single time point cannot reflect the degree of trauma. In fact, with excessive destruction of acinar cells in severe pancreatic trauma, but amylase levels are reduced. The degree of trauma needs to be assessed with reference to multiple indicators at different time points. (5) After modeling, with the increase of IL-6 and TNF-α, IL-10 increased to a certain extent. As a negative feedback regulator, IL-10 plays an important role in the pro-inflammatory/anti-inflammatory balance, and its elevation may be a defensive response of the body [20,21]. However, with the initiation of inflammatory cascades by pro-inflammatory cytokine, anti-inflammatory cytokine IL-10 was inhibited and gradually decreased. (6) After 72 h of continuous observation, at 6, 24, 48, and 72 h timepoints in 3 cm^2 trauma subgroups, with ascites reabsorption, ascites volume decreased and serum potassium recovered. The decrease of wet weight of pancreas may be attribute to the pancreatic duct rupture and pancreatic leakage. In addition, serum anti-inflammatory cytokine, serum calcium decreased and serum pro-inflammatory cytokine and ascitic amylase and lipase increased, indicating that damage tended to worsen. We consider that this is due to the presence of pancreatic duct rupture and pancreatic leakage in this pancreatic trauma model, and the pancreatic juice containing a large amount of amylase and lipase entered the abdominal cavity to corrode the intra-abdominal organs and caused

secondary infection of the abdominal cavity.

In conclusion, we developed a multifunctional impactor and successfully established a pancreatic trauma model in rats based on controlling the injury area. Compared to the previous pancreatic trauma model established by airstream impact, in addition to ensuring the stability and validity of the model, the damage area and strength range of the model can be adjusted more widely. Both 3 cm^2 and 6 cm^2 trauma groups can simulate severe pancreatic trauma, but in order to obtain a deeper injury assessment and carry out therapeutic research, 3 cm^2 trauma group with higher survival rate and longer survival time may be more suitable for rat model. We believe that the application of this model to the basic scientific research on pathophysiology, pathology, cell biology and molecular biology of pancreatic trauma should be produced multiple exciting discoveries, which will have a positive impact on the clinical treatment and management of pancreatic trauma. At the same time, there are still some shortcomings in this study: (1) The operation of the impactor is completed by manually pulling the operating rod because mechanical automation has not been achieved; (2) The measuring device of impact velocity is not currently captured; (3) More trauma assessments and more organ damage have not been addressed. Due to these issues, we will further improve and perfect this model in subsequent studies.

Authors' contributions

Wang Hailin and Han Li participated in the literature search, data collection, data analysis, data interpretation, and writing. Zhao Zhirong and Wang Qingqing participated in the study design, data collection, and writing. Li Jingdong participated in the study design, data collection, data analysis, and writing. Dai Ruiwu participated in the literature search, study design, data collection, data analysis, data interpretation, writing, and critical revision.

Funding statement

The study was supported by Science and Technology Cooperation Fund of Nanchong City and North Sichuan Medical College (No.19SXHZ0171); Hospital Management fund of the General Hospital of Western Theater Command (2021-XZYG-B16); the Sichuan Science and Technology Program (2022YFS0195).

Data availability statement

Data included in article/supplementary material/referenced in article.

Additional information

No additional information is available for this paper.

Declaration of competing interest

The authors declare that they have no known competing financial interests or personal relationships that could have appeared to influence the work reported in this paper.

Abbreviations

AAST: American Association for the Surgery of Trauma; SD: sprague-dawley; AMS: amylase; LPS: lipase; YPLL: years of potential life loss; HE: hematoxylin-eosin; CV: Coefficient of variation; IL-6/10: Interleukin-6/10; TNF-α: tumor necrosis factor-α; ELISA: enzyme-linked immunosorbent assay.

References

[1] A.R. Ayoob, et al., Pancreatic trauma: imaging review and management update, Radiographics 41 (1) (2021) 58–74.
[2] G.J. Jurkovich, C.J. Carrico, Pancreatic trauma, Surg. Clin. 70 (3) (1990) 575–593.
[3] D. Kollár, et al., [Diagnosis and management of blunt pancreatic trauma], Orv. Hetil. 159 (2) (2018) 43–52.
[4] B. Phillips, et al., A subgroup analysis of penetrating injuries to the pancreas: 777 patients from the National Trauma Data Bank, 2010-2014, J. Surg. Res. 225 (2018) 131–141.
[5] A.F. Schmiegelow, J.H. Stockholm, S.K. Burgdorf, [Traumatic pancreatic lesions], Ugeskr Laeger 181 (16) (2019).
[6] E.E. Moore, et al., Organ injury scaling, II: pancreas, duodenum, small bowel, colon, and rectum, J. Trauma 30 (11) (1990) 1427–1429.
[7] E.E. Moore, et al., Organ injury scaling: spleen and liver (1994 revision), J. Trauma 38 (3) (1995) 323–324.
[8] G.S. Raju, et al., Effect of a novel pancreatic stent design on short-term pancreatic injury in a canine model, Endoscopy 38 (3) (2006) 260–265.
[9] R. Hayda, R.M. Harris, C.D. Bass, Blast injury research: modeling injury effects of landmines, bullets, and bombs, Clin. Orthop. Relat. Res. (422) (2004) 97–108.
[10] R. Dai, et al., Establishment and characteristics of an animal model for isolated pancreatic trauma, J. Trauma Acute Care Surg. 73 (3) (2012) 648–653.
[11] D. Rui-Wu, et al., Cell cycle characteristics of the pancreas in an animal model of isolated pancreatic trauma, J. Trauma Acute Care Surg. 76 (3) (2014) 784–790.
[12] V. Brooks, NON-PENETRATING PANCREATIC TRAUMA, 13, West Indian Med J, 1964, pp. 84–89.
[13] C. Tănăsescu, D. Bratu, D. Sabău, Characteristics of thoraco-abdominal injuries - a series of three cases, Chirurgia (Bucur) 115 (4) (2020) 530–536.
[14] A.E. Walker, The adult pancreas in trauma and disease, Acad Forensic Pathol 8 (2) (2018) 192–218.

[15] J.G. Martin, et al., Evaluation and management of blunt solid organ trauma, Tech. Vasc. Intervent. Radiol. 20 (4) (2017) 230–236.
[16] S. Mohseni, et al., Outcomes after resection versus non-resection management of penetrating grade III and IV pancreatic injury: a trauma quality improvement (TQIP) databank analysis, Injury 49 (1) (2018) 27–32.
[17] W.B. Yang, et al., [The therapeutic experience of blunt pancreatic trauma], Zhonghua Wai Ke Za Zhi 57 (9) (2019) 660–665.
[18] M. Cully, J. Perry, M.O. Titus, An unlikely cause of a blunt pancreatic injury, Pediatr. Emerg. Care 35 (12) (2019) e238–e240.
[19] R. Sutton, Parenchymal pressure injury Ca(2+) entry mechanism in pancreatitis, Cell Calcium 88 (2020), 102208.
[20] A. Shemer, et al., Interleukin-10 prevents pathological microglia hyperactivation following peripheral endotoxin challenge, Immunity 53 (5) (2020) 1033–1049.e7.
[21] K.S. Park, et al., Mesenchymal stromal cell-derived nanovesicles ameliorate bacterial outer membrane vesicle-induced sepsis via IL-10, Stem Cell Res. Ther. 10 (1) (2019) 231.